

FreeMatch: Self-adaptive Thresholding for Semi-supervised Learning

Yidong Wang ^{*1} Hao Chen ^{*2} Qiang Heng ^{*3} Wenxin Hou ⁴ Marios Savvides ² Shinozaki Takahiro ¹
 Bhiksha Raj ² Zhen Wu ⁵ Jindong Wang ⁶

Abstract

Pseudo labeling and consistency regularization approaches with confidence-based thresholding have made great progress in semi-supervised learning (SSL). In this paper, we theoretically and empirically analyze the relationship between the unlabeled data distribution and the desirable confidence threshold. Our analysis shows that previous methods might fail to define favorable threshold since they either require a pre-defined / fixed threshold or an ad-hoc threshold adjusting scheme that does not reflect the learning effect well, resulting in inferior performance and slow convergence, especially for complicated unlabeled data distributions. We hence propose *FreeMatch* to define and adjust the confidence threshold in a self-adaptive manner according to the model’s learning status. To handle complicated unlabeled data distributions more effectively, we further propose a self-adaptive class fairness regularization method that encourages the model to produce diverse predictions during training. Extensive experimental results indicate the superiority of FreeMatch especially when the labeled data are extremely rare. FreeMatch achieves **5.78%**, **13.59%**, and **1.28%** error rate reduction over the latest state-of-the-art method FlexMatch on CIFAR-10 with 1 label per class, STL-10 with 4 labels per class, and ImageNet with 100k labels respectively.

1. Introduction

Despite the success of deep learning in various fields (He et al., 2016; Devlin et al., 2018; Dong et al., 2018), its superior performance heavily relies on supervised training with sufficient labeled data. However, a large amount of labeled

data are usually laborious and expensive to obtain. To alleviate the reliance on labeled data, semi-supervised learning (SSL) is developed to improve the model’s generalization performance by exploiting a massive amount of unlabeled data. Pseudo labeling (Lee et al., 2013; Xie et al., 2020b; McLachlan, 1975) and consistency regularization (Bachman et al., 2014; Samuli & Timo, 2017; Sajjadi et al., 2016) are two popular paradigms designed for modern SSL. Recently, the combinations of these two paradigms have shown promising results (Xie et al., 2020a; Sohn et al., 2020; Pham et al., 2021; Xu et al., 2021; Zhang et al., 2021). The key idea is that the model should produce similar predictions or the same pseudo labels for the same unlabeled data under different perturbations following the smoothness and low-density assumptions in SSL (Chapelle et al., 2006).

However, a drawback of these methods is that they either need a *fixed threshold* (Xie et al., 2020a; Sohn et al., 2020; Zhang et al., 2021) or an *ad-hoc threshold adjusting scheme* (Xu et al., 2021) to compute loss with only confident unlabeled samples. Specifically, UDA (Xie et al., 2020a) and FixMatch (Sohn et al., 2020) retain the fixed high threshold to ensure the quality of useful pseudo labels. However, one fixed high threshold for all unlabeled data could lead to low data utilization in the early training stage and ignore the different learning difficulties of different classes. Dash (Xu et al., 2021) proposes to gradually grow the fixed *global* (dataset-specific) threshold as the training progresses. Although the utilization of unlabeled data is improved, their ad-hoc threshold adjusting scheme is totally controlled by hyper-parameters and thus disconnects with model’s learning process. FlexMatch (Zhang et al., 2021) demonstrates that different classes should have different *local* (class-specific) thresholds based on the numbers of clean unlabeled data whose confidence is higher than a pre-defined global threshold. While the proposed local thresholds take the learning difficulties of different classes into account, they are still mapped from a pre-defined fixed global threshold. In a nutshell, these methods, considering either global or local threshold alone, might be incapable of adjusting thresholds according to the model’s actual learning status on unlabeled data, therefore impeding the learning process, especially when labeled data is too scarce to provide adequate supervision and reflect the unlabeled data distribution.

^{*}Equal contribution ¹Tokyo Institute of Technology. Work done when Yidong Wang was an intern at Microsoft Research Asia.

²Carnegie Mellon University ³North Carolina State University

⁴Microsoft STCA ⁵Nanjing University ⁶Microsoft Research Asia.

Correspondence to: Jindong Wang <jindwang@microsoft.com>.

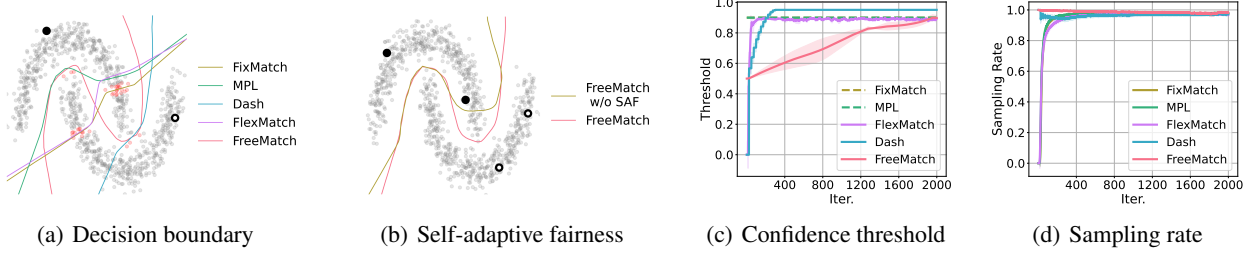


Figure 1. Demonstration of how FreeMatch works on “two-moon” dataset. We generate only 2 labeled data points (one label per each class, denoted by black dot and round circle) and 1,000 unlabeled data points (in gray) in 2-D space. We train a 3-layer MLP with 64 neurons in each layer and ReLU activation for 2,000 iterations. The red samples indicate the different samples whose confidence values are above the threshold of FreeMatch but below that of FixMatch. (a) Decision boundary of FreeMatch and other SSL methods. (b) Decision boundary improvement of self-adaptive fairness (SAF) on two labeled samples per class. (c) Class-average confidence threshold. (d) Class-average sampling rate of FreeMatch during training. The sampling rate is computed on unlabeled data as $\sum_b^{N_U} \mathbb{1}(\max(q_b) > \tau)/N_U$. We run the experiments for 5 times to compute the error bars.

For example, as shown in Figure 1(a), on the “two-moon” dataset with only 1 labeled sample for each class, the decision boundaries obtained by previous methods fail in the low-density assumption. Then, two questions naturally arise: 1) *Is it necessary to determine the threshold according to unlabeled data distribution?* and 2) *How to adaptively adjust the threshold with most training efficiency?*

In this paper, we theoretically and empirically analyze the relationship between the unlabeled data distribution and thresholds. Our theoretical analysis shows that different datasets and classes should determine their global (dataset-specific) and local (class-specific) thresholds according to the learning status. More specifically, we need a low global threshold to select more unlabeled data and speed up convergence at early training stages when the model cannot classify unlabeled data well. As the prediction confidence increases, a higher global threshold is necessary to filter out wrong pseudo labels to alleviate the confirmation bias (Arazo et al., 2020). Besides, local threshold should be defined on each class based on the learning difficulty and learning status. The “two-moon” dataset in Figure 1(a) illustrates that the decision boundary is most reasonable when considering the relationship between thresholds and the unlabeled data distribution.

Based on above analysis, we propose *FreeMatch* to adjust the thresholds in a self-adaptive manner according to the model predictions that reflect the learning difficulty and status of each class (Guo et al., 2017). Specifically, FreeMatch uses the self-adaptive thresholding (SAT) to estimate both the global (dataset-specific) and local thresholds (class-specific) via the exponential moving average (EMA) of the unlabeled data confidence. To handle barely supervised setting (Sohn et al., 2020) more effectively, we further propose a class fairness objective to encourage the model to produce diverse (i.e., fair) predictions among all classes (as shown

in Figure 1(b)). FreeMatch optimizes the fairness objective also in a self-adaptive fashion based on the EMA model predictions and the batch predictions. The overall training objective of FreeMatch maximizes the mutual information between model’s input and output (John Bridle, 1991), producing confident and diverse predictions on unlabeled data. Experimental results on SSL benchmarks validate its effectiveness over other state-of-the-art methods. To conclude, our contributions are:

- We theoretically analyze the interactions how unlabeled data distribution and thresholds affect unlabeled data utilization (sampling rate).
- Based on our theory, we discuss several interesting and important implications for guiding the choice of thresholds in SSL.
- We propose FreeMatch, a self-adaptive SSL method that is free of setting thresholds manually. Extensive experimental results show FreeMatch achieves superior results, especially when labeled data is very limited.

2. Theoretical Motivation

In this section, we characterize how unlabeled data distribution and threshold influence unlabeled data sampling rate. Then, we discuss some interesting and important implications. Note that our analysis is algorithm-agnostic that can be applied to both traditional and modern SSL algorithms.

We aim to demonstrate the necessity of the self-adaptability and increased granularity in the confidence thresholds for SSL. Inspired by (Yang & Xu, 2020), we consider a binary classification problem where the true distribution is an even mixture of two Gaussians (i.e., the label Y is equally likely to be positive (+1) or negative (-1)). The input X has the

following conditional distribution:

$$\begin{aligned} X \mid Y = -1 &\sim \mathcal{N}(\mu_1, \sigma_1^2), \\ X \mid Y = +1 &\sim \mathcal{N}(\mu_2, \sigma_2^2). \end{aligned} \quad (1)$$

We assume $\mu_2 > \mu_1$ without loss of generality. Suppose that our classifier outputs confidence score as:

$$s(x) = \frac{1}{1 + e^{-\beta(x - \frac{\mu_1 + \mu_2}{2})}}, \quad (2)$$

where β is a positive parameter that reflects the model learning status and it is expected to gradually grow during training as the model becomes more confident. Note that $\frac{\mu_1 + \mu_2}{2}$ is in fact the Bayes' optimal linear decision boundary. We consider the scenario where a fixed threshold $\tau \in (\frac{1}{2}, 1)$ is used to generate pseudo labels. A sample x is assigned pseudo label $+1$ if $s(x) > \tau$ and assigned pseudo label -1 if $s(x) < 1 - \tau$. The pseudo label is 0 (masked) if $1 - \tau \leq s(x) \leq \tau$.

Theorem 2.1. *For a binary classification problem as mentioned above, the pseudo label Y_p has the following probability distribution:*

$$\begin{aligned} P(Y_p = 1) &= \frac{1}{2} \Phi\left(\frac{\frac{\mu_2 - \mu_1}{2} - \frac{1}{\beta} \log\left(\frac{\tau}{1-\tau}\right)}{\sigma_2}\right) \\ &\quad + \frac{1}{2} \Phi\left(\frac{\frac{\mu_1 - \mu_2}{2} - \frac{1}{\beta} \log\left(\frac{\tau}{1-\tau}\right)}{\sigma_1}\right), \\ P(Y_p = -1) &= \frac{1}{2} \Phi\left(\frac{\frac{\mu_2 - \mu_1}{2} - \frac{1}{\beta} \log\left(\frac{\tau}{1-\tau}\right)}{\sigma_1}\right) \quad (3) \\ &\quad + \frac{1}{2} \Phi\left(\frac{\frac{\mu_1 - \mu_2}{2} - \frac{1}{\beta} \log\left(\frac{\tau}{1-\tau}\right)}{\sigma_2}\right), \\ P(Y_p = 0) &= 1 - P(Y_p = 1) - P(Y_p = -1), \end{aligned}$$

where Φ is the cumulative distribution function of a standard normal distribution. Moreover, $P(Y_p = 0)$ increases as $\mu_2 - \mu_1$ gets smaller.

Proof. See Appendix A. \square

Theorem 2.1 has the following implications:

- (i) Trivially, unlabeled data utilization (sampling rate) $1 - P(Y_p = 0)$ is directly controlled by threshold τ . As the confidence threshold τ gets larger, the unlabeled data utilization gets lower. At the early training stage, adopting a high threshold may lead to low sampling rate and slow convergence since β is still small. Besides, if τ stays fixed, as β grows, the sampling rate may rapidly increase at early training, which may introduce many wrong pseudo labels and impede learning.

- (ii) Perhaps more interestingly, $P(Y_p = 1) \neq P(Y_p = -1)$ if $\sigma_1 \neq \sigma_2$. In fact, the larger τ is, the more imbalanced the pseudo labels are. This is undesirable in the sense that we aim to tackle a balanced classification problem. Imbalanced pseudo labels may distort the decision boundary and lead to the so-called pseudo label bias. An easy remedy for this is to use class-specific thresholds τ_2 and $1 - \tau_1$ to assign pseudo labels.
- (iii) The sampling rate $1 - P(Y_p = 0)$ decreases as $\mu_2 - \mu_1$ gets smaller: the more similar the two classes are, the more likely that an unlabeled sample will be masked. As the two classes gets more similar, there would be more samples mixed in feature space where the model is less confidence about its predictions, thus a moderate threshold is needed to balance the sampling rate.

Guided by Theorem 2.1, we propose that at the early training stages, τ should be low to encourage diverse pseudo labels, improve unlabeled data utilization and fasten convergence. However, as training continues and β grows larger, a consistently low threshold will lead to unacceptable confirmation bias. Ideally, the threshold τ should increase along with β to maintain a stable sampling rate throughout. Since different classes have different levels of intra-class diversity (different σ) and some classes are harder to classify than others ($\mu_2 - \mu_1$ is small), a fine-grained *class-specific* threshold is desirable to encourage fair assignment of pseudo labels to different classes. The challenge is how to design a threshold adjusting scheme that takes all implications into account, which is the main contribution of this paper. We demonstrate our algorithm by plotting the average threshold trend and marginal pseudo label probability (i.e. sampling rate) during training in Figure 1(c) and 1(d). To sum up, we should determine the global (dataset-specific) and local (class-specific) thresholds by estimating the learning status via predictions from the model. We then describe the details of our method.

3. Preliminary

In SSL, the training data consists of labeled and unlabeled data. Let $\mathcal{D}_L = \{(x_b, y_b) : b \in [N_L]\}$ and $\mathcal{D}_U = \{u_b : b \in [N_U]\}$ ¹ be the labeled and unlabeled data, where N_L and N_U is their number of samples, respectively. The supervised loss for labeled data is:

$$\mathcal{L}_s = \frac{1}{B} \sum_{b=1}^B \mathcal{H}(y_b, p_m(y|\omega(x_b))), \quad (4)$$

where B is the batch size, $\mathcal{H}(\cdot, \cdot)$ refers to cross-entropy loss, $\omega(\cdot)$ means the stochastic data augmentation function, and $p_m(\cdot)$ is the output probability from the model.

An intuitive approach to leverage unlabeled data is to maxi-

¹ $[N] := \{1, 2, \dots, N\}$.

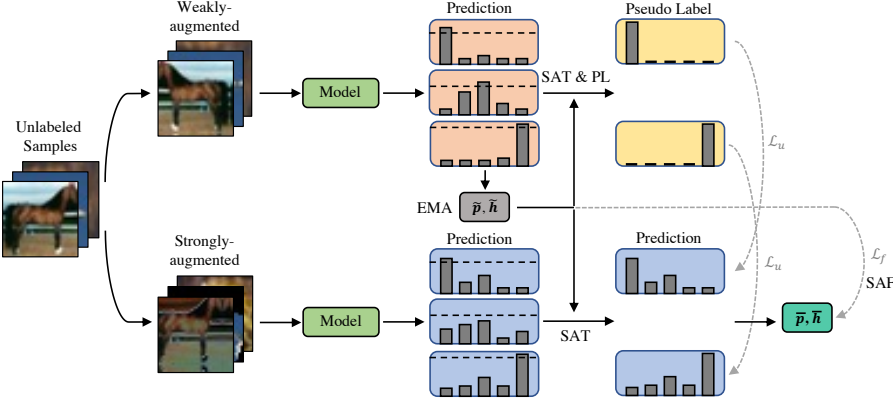


Figure 2. Pipeline diagram of FreeMatch. The weakly-augmented unlabeled samples (top) are fed into the model to obtain predictions (orange box), and similarly for strong-augmented unlabeled samples (bottom and blue box). We use self-adaptive threshold (SAT) computed from the EMA of prediction statistics from weakly-augmented samples to select sufficiently confident samples to compute \mathcal{L}_u . We also compute the self-adaptive fairness loss \mathcal{L}_f on the expected predictions on strongly augmented samples.

imize the mutual information between the model’s input and output on unlabeled data (John Bridle, 1991):

$$\mathcal{I}(y, x) = H(\mathbb{E}_u [p_m(y|u)]) - \mathbb{E}_u [H(p_m(y|u))], \quad (5)$$

where \mathbb{E}_u is the expectation over \mathcal{D}_U and $H(\cdot)$ denotes entropy. The first term corresponds to fairness on each class as mentioned in (John Bridle, 1991) and the second term denotes entropy minimization (Grandvalet et al., 2005) which makes the unlabeled data decisiveness and model’s decision boundary lies in low-density regime (Chapelle et al., 2006).

In this work, we focus on pseudo labeling using cross-entropy loss with confidence threshold for entropy minimization. We also adopt the “Weak and Strong Augmentation” strategy introduced by UDA (Xie et al., 2020a). Formally, the unsupervised training objective for unlabeled data is:

$$\mathcal{L}_u = \frac{1}{\mu B} \sum_{b=1}^{\mu B} \mathbb{1}(\max(q_b) > \tau) \cdot \mathcal{H}(\hat{q}_b, Q_b). \quad (6)$$

We use q_b and Q_b to denote abbreviation of $p_m(y|\omega(u_b))$ and $p_m(y|\Omega(u_b))$, respectively. \hat{q}_b is the hard “one-hot” label converted from q_b , μ is the ratio of unlabeled data batch size to labeled data batch size, and $\mathbb{1}(\cdot > \tau)$ is the indicator function for confidence-based thresholding with τ being the threshold. The weak augmentation (i.e., random crop and flip) and strong augmentation (i.e., RandAugment (Cubuk et al., 2020)) is represented by $\omega(\cdot)$ and $\Omega(\cdot)$ respectively.

The fairness objective \mathcal{L}_f is used to encourage the model to predict each class at the same frequency, which is usually in the form of $\mathcal{L}_f = \mathbf{U} \log \mathbb{E}_{\mu B} [q_b]$ (Andreas Krause, 2010), where \mathbf{U} stands for a uniform prior distribution. One may notice that using a uniform prior not only prevents the scalability of non-uniform data distribution but also ignores the

fact that underlying pseudo label distribution for mini-batch may be imbalanced due to the sampling mechanism.

4. FreeMatch

Inspired by our analysis above, we propose *FreeMatch* to adaptively compute the threshold by taking advantage of distributions for the unlabeled data.

4.1. Self-Adaptive Thresholding

Based on our analysis in Section 2, the key to determining thresholds for SSL is that thresholds should reflect the learning status. The learning effect can be estimated by the prediction confidence of a well-calibrated model (Guo et al., 2017). Hence, we propose *self-adaptive thresholding* (SAT) that automatically defines and adaptively adjusts the confidence threshold for each class by leveraging the model predictions during training. SAT first estimates a global threshold as the EMA of the confidence from the model. Then, SAT modulates the global threshold via the local class-specific threshold estimated as the EMA of the probability for each class from the model. When training starts, the threshold is low to accept more possibly correct samples into training. As the model becomes more confident, the threshold adaptively increases to filter out possibly incorrect samples to reduce the confirmation bias and pseudo label bias. Therefore, we define SAT as $\tau_t(c)$ indicating the threshold for class c at t -th iteration.

Self-adaptive Global Threshold There are several desirable properties of the global threshold based on the theoretical analysis. At first, the global threshold in SAT should be related to the model’s confidence on unlabeled data, reflecting the overall learning status. Moreover, the global

threshold should stably increase during training to ensure incorrect pseudo labels are discarded. We design the global threshold τ_t as average confidence from the model on unlabeled data, where t represents the t -th time step (iteration). However, it would be time-consuming to compute the confidence for all unlabeled data at every time step or even every training epoch due to its large volume. Instead, we estimate the global confidence as the exponential moving average (EMA) of the confidence at each training time step. We initialize τ_t as $\frac{1}{C}$ where C indicates the number of classes. The global threshold τ_t is defined and adjusted as:

$$\tau_t = \begin{cases} \frac{1}{C}, & \text{if } t = 0, \\ \lambda\tau_{t-1} + (1 - \lambda)\frac{1}{\mu B} \sum_{b=1}^{\mu B} \max(q_b), & \text{otherwise,} \end{cases} \quad (7)$$

where $\lambda \in (0, 1)$ is the momentum decay of EMA.

Self-adaptive Local Threshold The local threshold is to modulate the global threshold in a class-specific fashion to account for the intra-class diversity. We compute the expectation of the model’s predictions on each class c to estimate the class-specific learning status:

$$\tilde{p}_t(c) = \begin{cases} \frac{1}{C}, & \text{if } t = 0, \\ \lambda\tilde{p}_{t-1}(c) + (1 - \lambda)\frac{1}{\mu B} \sum_{b=1}^{\mu B} q_b(c), & \text{otherwise,} \end{cases} \quad (8)$$

where $\tilde{p}_t = [\tilde{p}_t(1), \tilde{p}_t(2), \dots, \tilde{p}_t(C)]$ is the list containing all $\tilde{p}_t(c)$. Integrating the global and local thresholds, we obtain the final self-adaptive threshold $\tau_t(c)$ as:

$$\begin{aligned} \tau_t(c) &= \text{MaxNorm}(\tilde{p}_t(c)) \cdot \tau_t \\ &= \frac{\tilde{p}_t(c)}{\max\{\tilde{p}_t(c) : c \in [C]\}} \cdot \tau_t, \end{aligned} \quad (9)$$

where MaxNorm is the Maximum Normalization (i.e., $x' = \frac{x}{\max(x)}$). Finally, the unsupervised training objective \mathcal{L}_u at t -th iteration is:

$$\mathcal{L}_u = \frac{1}{\mu B} \sum_{b=1}^{\mu B} \mathbb{1}(\max(q_b) > \tau_t(\arg \max(q_b)) \cdot \mathcal{H}(\hat{q}_b, Q_b)). \quad (10)$$

4.2. Self-Adaptive Fairness

We include the class fairness objective as mentioned in Section 3 into FreeMatch to encourage the model to make diverse predictions for each class and thus produce meaningful self-adaptive threshold, especially under the settings where labeled data are rare. Instead of using a uniform prior as in (Arazo et al., 2020), we use the EMA of model predictions \tilde{p}_t from Eq. (8) as an estimate of the expectation of prediction distribution over unlabeled data. We optimize the cross-entropy of \tilde{p}_t and $\bar{p} = \mathbb{E}_{\mu B}[p_m(y|\Omega(u_b))]$ over

mini-batch as an estimate of $H(\mathbb{E}_u[p_m(y|u)])$. Considering that the underlying pseudo label distribution may not be uniform, we propose to modulate the fairness objective in a self-adaptive way, i.e., normalizing the expectation of probability by the histogram distribution of pseudo labels to counter the negative effect of imbalance as:

$$\begin{aligned} \bar{p} &= \frac{1}{\mu B} \sum_{b=1}^{\mu B} \mathbb{1}(\max(q_b) \geq \tau_t(\arg \max(q_b)) Q_b, \\ \bar{h} &= \text{Hist}_{\mu B} \left(\mathbb{1}(\max(q_b) \geq \tau_t(\arg \max(q_b)) \hat{Q}_b) \right). \end{aligned} \quad (11)$$

Similar to \tilde{p}_t , we compute \tilde{h}_t as:

$$\tilde{h}_t = \lambda\tilde{h}_{t-1} + (1 - \lambda) \text{Hist}_{\mu B}(\hat{q}_b). \quad (12)$$

The self-adaptive fairness (SAF) \mathcal{L}_f at t -th iteration is formulated as:

$$\mathcal{L}_f = -\mathcal{H} \left(\text{SumNorm} \left(\frac{\tilde{p}_t}{\tilde{h}_t} \right), \text{SumNorm} \left(\frac{\bar{p}}{\bar{h}} \right) \right), \quad (13)$$

where $\text{SumNorm} = \frac{(\cdot)}{\sum(\cdot)}$. SAF encourages the expectation of the output probability for each mini-batch to be close to a marginal class distribution of the model, after normalized by histogram distribution. It helps the model produce diverse predictions especially for barely supervised settings (Sohn et al., 2020), and therefore converges faster and generalizes better. This is also illustrated in Figure 1(b).

The overall objective for FreeMatch at t -th iteration is:

$$\mathcal{L} = \mathcal{L}_s + w_u \mathcal{L}_u + w_f \mathcal{L}_f, \quad (14)$$

where w_u and w_f represents the loss weight for \mathcal{L}_u and \mathcal{L}_f respectively. With \mathcal{L}_u and \mathcal{L}_f , FreeMatch maximizes the mutual information between its outputs and inputs. The overall model pipeline is shown in Figure 2. We also present the procedure of FreeMatch in Algorithm 1 in Appendix.

5. Experiments

5.1. Setup

We evaluate FreeMatch on common benchmarks: CIFAR-10/100 (Krizhevsky et al., 2009), SVHN (Netzer et al., 2011), STL-10 (Coates et al., 2011) and ImageNet (Deng et al., 2009). Following previous work (Sohn et al., 2020; Xu et al., 2021; Zhang et al., 2021), we conduct experiments with varying amounts of labeled data. In addition to the commonly-chosen labeled amounts, following (Sohn et al., 2020), we further include the most challenging case of CIFAR-10: each class has only *one* labeled sample.

For a fair comparison, we train and evaluate all methods using the unified codebase TorchSSL (Zhang et al., 2021)²

²<https://github.com/TorchSSL/TorchSSL>

Table 1. Error rates on CIFAR-10/100, SVHN, and STL-10 datasets. The fully-supervised results of STL-10 are unavailable since we do not have label information for its unlabeled data. **Bold** indicates the best result and underline indicates the second-best result.

Dataset	CIFAR-10				CIFAR-100			SVHN			STL-10	
	10	40	250	4000	400	2500	10000	40	250	1000	40	1000
II Model (2015)	79.18 \pm 1.11	74.34 \pm 1.76	46.24 \pm 1.29	13.13 \pm 0.59	86.96 \pm 0.80	58.80 \pm 0.66	36.65 \pm 0.00	67.48 \pm 0.95	13.30 \pm 1.12	7.16 \pm 0.11	74.31 \pm 0.85	32.78 \pm 0.40
Pseudo Label (2013)	80.21 \pm 0.55	74.61 \pm 0.26	46.49 \pm 2.20	15.08 \pm 0.19	87.45 \pm 0.85	57.74 \pm 0.28	36.55 \pm 0.24	64.61 \pm 5.6	15.59 \pm 0.95	9.40 \pm 0.32	74.68 \pm 0.99	32.64 \pm 0.71
VAT (2018)	79.81 \pm 1.17	74.66 \pm 2.12	41.03 \pm 1.79	10.51 \pm 0.12	85.20 \pm 1.40	46.84 \pm 0.79	32.14 \pm 0.19	74.75 \pm 3.38	4.33 \pm 0.12	4.11 \pm 0.20	74.74 \pm 0.38	37.95 \pm 1.12
Mean Teacher (2017)	76.37 \pm 0.44	70.09 \pm 1.60	37.46 \pm 3.30	8.10 \pm 0.21	81.11 \pm 1.44	45.17 \pm 1.06	31.75 \pm 0.23	36.09 \pm 3.98	3.45 \pm 0.03	3.27 \pm 0.05	71.72 \pm 1.45	33.90 \pm 1.37
UDA (2020a)	34.53 \pm 10.69	10.62 \pm 3.75	5.16 \pm 0.06	4.29 \pm 0.07	46.39 \pm 1.59	27.73 \pm 0.21	22.49 \pm 0.23	5.12 \pm 4.27	1.92 \pm 0.05	1.89 \pm 0.01	37.42 \pm 8.44	6.64 \pm 0.17
FixMatch (2020)	24.79 \pm 7.65	7.47 \pm 0.28	4.86 \pm 0.05	4.21 \pm 0.08	46.42 \pm 0.82	28.03 \pm 0.16	22.20 \pm 0.12	3.81 \pm 1.18	2.02 \pm 0.02	<u>1.96</u> \pm 0.03	35.97 \pm 4.14	6.25 \pm 0.33
Dash (2021)	27.28 \pm 14.09	8.93 \pm 3.11	5.16 \pm 0.23	4.36 \pm 0.11	44.82 \pm 0.96	27.15 \pm 0.22	21.88 \pm 0.07	<u>2.19</u> \pm 0.18	2.04 \pm 0.02	1.97 \pm 0.01	34.52 \pm 4.30	6.39 \pm 0.56
MPL (2021)	23.55 \pm 6.01	6.62 \pm 0.91	5.76 \pm 0.24	4.55 \pm 0.04	46.26 \pm 1.84	27.71 \pm 0.19	<u>21.74</u> \pm 0.09	9.33 \pm 8.02	2.29 \pm 0.04	2.28 \pm 0.02	35.76 \pm 4.83	6.66 \pm 0.00
FlexMatch (2021)	<u>13.85</u> \pm 12.04	<u>4.97</u> \pm 0.06	4.98 \pm 0.09	<u>4.19</u> \pm 0.01	<u>39.94</u> \pm 1.62	<u>26.49</u> \pm 0.20	21.90 \pm 0.15	8.19 \pm 3.20	6.59 \pm 2.29	6.72 \pm 0.30	<u>29.15</u> \pm 4.16	<u>5.77</u> \pm 0.18
FreeMatch	8.07 \pm 4.24	4.90 \pm 0.04	4.88 \pm 0.18	4.10 \pm 0.02	37.98 \pm 0.42	26.47 \pm 0.20	21.68 \pm 0.03	1.97 \pm 0.02	<u>1.97</u> \pm 0.01	<u>1.96</u> \pm 0.03	15.56 \pm 0.55	5.63 \pm 0.15
Fully-Supervised			4.62 \pm 0.05				19.30 \pm 0.09			2.13 \pm 0.01		-

with the same backbones and hyperparameters. Concretely, we use Wide ResNet-28-2 (Zagoruyko & Komodakis, 2016) for CIFAR-10, Wide ResNet-28-8 for CIFAR-100, Wide ResNet-37-2 (Zhou et al., 2020) for STL-10, and ResNet-50 (He et al., 2016) for ImageNet. We use SGD with a momentum of 0.9 as optimizer. The initial learning rate is 0.03 with a cosine learning rate decay schedule as $\eta = \eta_0 \cos(\frac{7\pi k}{16K})$, where η_0 is the initial learning rate, $k(K)$ is the current (total) training step and we set $K = 2^{20}$ for all datasets. At the testing phase, we use an exponential moving average with the momentum of 0.999 of the training model to conduct inference for all algorithms. The batch size of labeled data is 64 except for ImageNet where we set 128. We use the same weight decay value, pre-defined threshold τ , unlabeled batch ratio μ and loss weights introduced for Pseudo-Label (Lee et al., 2013), II model (Rasmus et al., 2015), Mean Teacher (Tarvainen & Valpola, 2017), VAT (Miyato et al., 2018), UDA (Xie et al., 2020a), FixMatch (Sohn et al., 2020), and FlexMatch (Zhang et al., 2021).

We implement MPL based on UDA as in (Pham et al., 2021), where we set temperature as 0.8 and w_u as 10. We do not fine-tune MPL on labeled data as in (Pham et al., 2021) since we find fine-tuning will make the model overfit the labeled data especially with very few of them. For Dash, we use the same parameters as in (Xu et al., 2021) except we warm-up on labeled data for 2 epochs since too much warm-up will lead to the overfitting (i.e. 2,048 training iterations). For FreeMatch, we set $w_u = 1$ for all experiments. Besides, we set $w_f = 0.01$ for CIFAR-10 with 10 labels, CIFAR-100 with 400 labels, STL-10 with 40 labels, ImageNet with 100k labels, and all experiments for SVHN. For other settings, we use $w_f = 0.05$. For SVHN, we find that using a low threshold at early training stage impedes the model to cluster the unlabeled data, thus we adopt two training techniques for SVHN: (1) warm-up the model on only labeled data for 2 epochs as Dash; and (2) restrict the SAT within the range [0.9, 0.95]. The detailed hyperparameters are introduced in Appendix C. We train each algorithm 3 times using different random seeds. The best error rates of all checkpoints are

Table 2. Error rates and running time on ImageNet classification task with 100k labels (i.e., 100 labels per class).

	Top1	Top5	Running Time (s/iter)
FixMatch	43.66	21.80	0.4
FlexMatch	41.85	19.48	0.6
FreeMatch	40.57	18.77	0.4

reported in the main text and the mean error rates of the last 20 checkpoints are reported in Appendix D.2.

5.2. Quantitative Results

The Top-1 classification error rates of CIFAR-10/100, SVHN, and STL-10 are reported in Table 1. The results on ImageNet with 100k labels (i.e., 100 labels per class) are in Table 2. We also provide detailed results on precision, recall, F1 score, and confusion matrix in Appendix D.2. These quantitative results demonstrate that FreeMatch achieves the best performance on CIFAR-10, CIFAR-100, STL-10, and ImageNet datasets, and it produces very close results on SVHN to the best competitor. On ImageNet with 100k labels, FreeMatch significantly outperforms the latest counterpart FlexMatch by **1.28%**³. We also notice that FreeMatch exhibits fast computation in ImageNet from Table 2. Note that FlexMatch is much slower than FixMatch and FreeMatch because it needs to maintain a list that records whether each sample is clean, which needs heavy indexing computation budget on large datasets.

Noteworthy is that, FreeMatch consistently outperforms other methods by a large margin on settings with *extremely limited labeled data*: **5.78%** on CIFAR-10 with 10 labels, **1.96%** on CIFAR-100 with 400 labels, and surprisingly **13.59%** on STL-10 with 40 labels. STL-10 is a more realistic and challenging dataset compared to others, which

³Following (Zhang et al., 2021), we train ImageNet for 2^{20} iterations like other datasets for a fair comparison. We use 4 Tesla V100 GPUs on ImageNet.

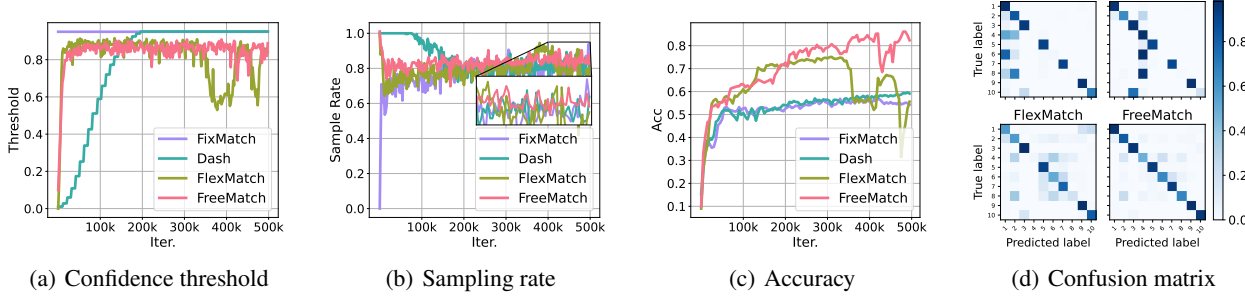


Figure 3. Demonstration of how FreeMatch works in STL-10 with 40 labels, compared to previous methods. (a) Class-average confidence threshold; (b) class-average sampling rate; (c) convergence speed in terms of accuracy; (d) confusion matrix, where the fading color of diagonal elements refers to the disparity of the accuracy.

consists of a large unlabeled set of 100k images. The significant improvements demonstrate the capability and potential of FreeMatch to be deployed in real-world applications.

5.3. Qualitative Analysis

We present some qualitative analysis: Why and how does FreeMatch work? What other benefits does it bring?

We evaluate the class average threshold and average sampling rate on STL-10 (40) (i.e., 40 labeled samples on STL-10) of FreeMatch to demonstrate how it works aligning with our theoretical analysis. We record the threshold and compute the sampling rate for each batch during training. The sampling rate is calculated on unlabeled data as $\frac{\sum_b^{\mu_B} \mathbb{1}(\max(q_b) > \tau_t(\arg \max(q_b)))}{\mu_B}$. We also plot the convergence speed in terms of accuracy and the confusion matrix to show the proposed component in FreeMatch helps improve performance. From Figure 3(a) and Figure 3(b), one can observe that the threshold and sampling rate change of FreeMatch is mostly consistent with our theoretical analysis. That is, at the early stage of training, the threshold of FreeMatch is relatively lower, compared to FlexMatch and FixMatch, resulting in higher unlabeled data utilization (sampling rate), which fastens the convergence. As the model learns better and becomes more confident, the threshold of FreeMatch increases to a high value to alleviate the confirmation bias, leading to stably high sampling rate. Correspondingly, the accuracy of FreeMatch increases vastly (as shown in Figure 3(c)) and resulting better class-wise accuracy (as shown in Figure 3(d)). Note that Dash fails to learn properly due to the employment of the high sampling rate until 100k iterations.

To further demonstrate the effectiveness of the class-specific threshold in FreeMatch, we present the T-SNE (Van der Maaten & Hinton, 2008) visualization of features of FlexMatch and FreeMatch on STL-10 (40) in Figure 4. We exhibit the corresponding local threshold for each class. In-

Table 3. Error rates of different threshold scheme compared with FixMatch (τ) and FlexMatch ($\tau * \mathcal{M}(\beta(c))$).

Threshold	CIFAR-10 (40)
τ (FixMatch)	7.47 ± 0.28
$\tau * \mathcal{M}(\beta(c))$ (FlexMatch)	4.97 ± 0.06
$\tau * \text{MaxNorm}(\tilde{p}_t(c))$	5.13 ± 0.03
τ_t (Global)	6.06 ± 0.65
$\tau_t * \mathcal{M}(\beta(c))$	8.40 ± 2.49
SAT (Global and Local)	4.92 ± 0.04

terestingly, FlexMatch has a high threshold, i.e., pre-defined 0.95, for class 0 and class 6, yet their feature variances are very large and are confused with other classes. This means the class-wise thresholds in FlexMatch cannot actually reflect the learning status. In contrast, FreeMatch clusters most classes better, thanks to SAT and SAF. Besides, for the similar classes 1, 3, 5, 7 that are confused with each other in T-SNE feature space, FreeMatch retains a higher average threshold 0.87 than 0.84 of FlexMatch, enabling FreeMatch to mask more wrong pseudo labels for confusing classes. The worse feature space of FlexMatch might cause the learning collapse at around 300k iterations.

5.4. Ablation Study

Self-adaptive Threshold We conduct experiments on the components of SAT in FreeMatch, and compare to the components in FlexMatch (Zhang et al., 2021) and FixMatch (Sohn et al., 2020). Specifically, we compare the performance of SSL algorithms using pseudo labeling and “strong-weak” augmentation strategy with different combinations of components in SAT and threshold adjusting scheme CPL in FlexMatch (Zhang et al., 2021) on CIFAR-10 (40), as shown in Table 3. We use τ indicates the fixed threshold in FixMatch, $\mathcal{M}(\beta(c))$ indicates the CPL in FlexMatch, τ_t denotes the global threshold, and $\text{MaxNorm}(\tilde{p}_t(c))$ denotes the local threshold proposed. SAT achieves the best per-

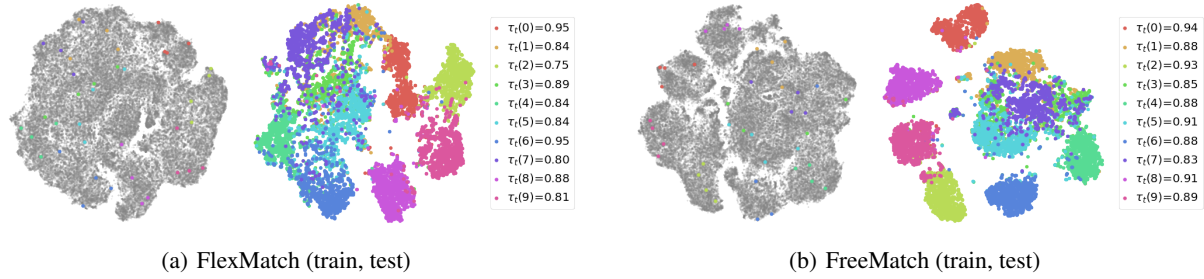


Figure 4. T-SNE visualization of FlexMatch and FreeMatch features on STL-10 (40). Unlabeled data is indicated by gray color. Local threshold $\tau_t(c)$ for each class is shown on the legend.

Table 4. Error rates of different class fairness regularization to show the ablation of self-adaptive fairness L_f (SAF).

Fairness	CIFAR-10 (10)
w/o fairness	10.37 ± 7.70
$U \log \bar{p}$	9.57 ± 6.67
$U \log \text{SumNorm}(\frac{\bar{p}}{h})$	12.07 ± 5.23
SAF	8.07 ± 4.24

formance among all the threshold schemes. Self-adaptive global threshold and local threshold themselves also achieve comparable results, compared to the fixed threshold, demonstrating both local and global threshold proposed are good learning effect estimators, which aligns to our theoretical analysis. When using CPL to adjust τ_t , the result is worse than the fixed threshold and exhibits significantly larger variance, indicating potential instability of CPL. Note that we did not include L_f in this ablation for a fair comparison.

Self-adaptive Fairness. As illustrated in Table 4, we also empirically study the effect of SAF on CIFAR-10 (10 labels). We study the original version of fairness objective as in (Arazo et al., 2020). Based on that, we study the operation of normalization probability by histograms and show that countering the effect of imbalanced underlying distribution indeed helps the model to learn and diverse better. One may notice that adding original fairness regularization alone already helps improve the performance as CIFAR-10 is class-balanced. Whereas adding normalization operation in the log operation hurts the performance, suggesting the underlying batch data are indeed not uniformly distributed.

6. Related Work

Self-training has been widely adopted in SSL, e.g., II model, MeanTeacher, MixMatch, ReMixMatch (Rasmus et al., 2015; Tarvainen & Valpola, 2017; Berthelot et al., 2019b;a; Xie et al., 2020a). The overall idea is to directly treat the model’s output probabilities as artificial soft labels for unlabeled data. Pseudo labeling is a variant of self-training that converts probabilities to hard “one-hot” labels (Lee et al., 2013; Sohn et al., 2020). Consistency regularization is applied to force the model’s predictions on the perturbed

versions of unlabeled data to be similar to the pseudo labels.

However, pseudo labels can be wrong and hurt the model’s generalization ability if they are included in the training, which is known as the confirmation bias (Arazo et al., 2020). To reduce confirmation bias, confidence-based thresholding techniques are proposed to ensure the quality of pseudo labels (Xie et al., 2020a; Sohn et al., 2020; Zhang et al., 2021; Xu et al., 2021), where only the unlabeled data whose confidences are higher than the threshold are retained. UDA (Xie et al., 2020a) and FixMatch (Sohn et al., 2020) keep the fixed pre-defined threshold during training. FlexMatch (Zhang et al., 2021) adjusts the pre-defined threshold in a class-specific fashion according to the per-class learning status estimated by the number of confident unlabeled data. Besides, Dash (Xu et al., 2021) defines a threshold according to the loss on labeled data and adjusts the threshold according to a fixed mechanism.

Except consistency regularization, entropy-based regularization is also used in SSL. Entropy minimization (Grandvalet et al., 2005) encourages the model to make confident predictions for all samples disregarding the actual class predicted, according to the low-density assumption in SSL. Maximization of expectation of entropy (Andreas Krause, 2010; Arazo et al., 2020) over all samples is also proposed to induce fairness to the model, enforcing the model to predict each class at the same frequency. But previous ones assume a uniform prior for underlying data distribution and also ignore the batch data distribution. Distribution alignment (Berthelot et al., 2019a) adjusts the pseudo labels according to labeled data distribution and the EMA of model predictions.

7. Conclusion

In this paper, we proposed FreeMatch, an SSL method to leverage the unlabeled data distribution for self-adaptive thresholding. We further proposed self-adaptive fairness to handle the barely supervised setting. FreeMatch outperforms other baselines across a variety of SSL benchmarks. We plan to develop better ways to alleviate the confirmation bias other than confidence-based thresholding techniques.

References

Andreas Krause, Pietro Perona, R. G. Discriminative clustering by regularized information maximization. In *Advances in neural information processing systems*, 2010.

Arazo, E., Ortego, D., Albert, P., O'Connor, N. E., and McGuinness, K. Pseudo-labeling and confirmation bias in deep semi-supervised learning. In *2020 International Joint Conference on Neural Networks (IJCNN)*, pp. 1–8. IEEE, 2020.

Bachman, P., Alsharif, O., and Precup, D. Learning with pseudo-ensembles. *Advances in neural information processing systems*, 27:3365–3373, 2014.

Berthelot, D., Carlini, N., Cubuk, E. D., Kurakin, A., Sohn, K., Zhang, H., and Raffel, C. Remixmatch: Semi-supervised learning with distribution matching and augmentation anchoring. In *International Conference on Learning Representations*, 2019a.

Berthelot, D., Carlini, N., Goodfellow, I., Papernot, N., Oliver, A., and Raffel, C. A. Mixmatch: A holistic approach to semi-supervised learning. *Advances in Neural Information Processing Systems*, 32, 2019b.

Carlini, N., Erlingsson, U., and Papernot, N. Distribution density, tails, and outliers in machine learning: Metrics and applications. *arXiv preprint arXiv:1910.13427*, 2019.

Chapelle, O., Schölkopf, B., and Zien, A. (eds.). *Semi-Supervised Learning*. The MIT Press, 2006.

Coates, A., Ng, A., and Lee, H. An analysis of single-layer networks in unsupervised feature learning. In *Proceedings of the fourteenth international conference on artificial intelligence and statistics*, pp. 215–223. JMLR Workshop and Conference Proceedings, 2011.

Cubuk, E. D., Zoph, B., Shlens, J., and Le, Q. V. Randaugment: Practical automated data augmentation with a reduced search space. In *Proceedings of the IEEE/CVF Conference on Computer Vision and Pattern Recognition Workshops*, pp. 702–703, 2020.

Deng, J., Dong, W., Socher, R., Li, L.-J., Li, K., and Fei-Fei, L. Imagenet: A large-scale hierarchical image database. In *2009 IEEE conference on computer vision and pattern recognition*, pp. 248–255. Ieee, 2009.

Devlin, J., Chang, M.-W., Lee, K., and Toutanova, K. Bert: Pre-training of deep bidirectional transformers for language understanding. *arXiv preprint arXiv:1810.04805*, 2018.

Dong, L., Xu, S., and Xu, B. Speech-transformer: a no-recurrence sequence-to-sequence model for speech recognition. In *2018 IEEE International Conference on Acoustics, Speech and Signal Processing (ICASSP)*, pp. 5884–5888. IEEE, 2018.

Grandvalet, Y., Bengio, Y., et al. Semi-supervised learning by entropy minimization. volume 367, pp. 281–296, 2005.

Guo, C., Pleiss, G., Sun, Y., and Weinberger, K. Q. On calibration of modern neural networks. In *International Conference on Machine Learning*, pp. 1321–1330. PMLR, 2017.

He, K., Zhang, X., Ren, S., and Sun, J. Deep residual learning for image recognition. In *Proceedings of the IEEE conference on computer vision and pattern recognition*, pp. 770–778, 2016.

John Bridle, Anthony Heading, D. M. Unsupervised classifiers, mutual information and 'phantom targets'. 1991.

Krizhevsky, A. et al. Learning multiple layers of features from tiny images. 2009.

Langley, P. Crafting papers on machine learning. In Langley, P. (ed.), *Proceedings of the 17th International Conference on Machine Learning (ICML 2000)*, pp. 1207–1216, Stanford, CA, 2000. Morgan Kaufmann.

Lee, D.-H. et al. Pseudo-label: The simple and efficient semi-supervised learning method for deep neural networks. In *Workshop on challenges in representation learning, ICML*, volume 3, pp. 896, 2013.

McLachlan, G. J. Iterative reclassification procedure for constructing an asymptotically optimal rule of allocation in discriminant analysis. *Journal of the American Statistical Association*, 70(350):365–369, 1975.

Miyato, T., Maeda, S.-i., Koyama, M., and Ishii, S. Virtual adversarial training: a regularization method for supervised and semi-supervised learning. *IEEE transactions on pattern analysis and machine intelligence*, 41(8):1979–1993, 2018.

Netzer, Y., Wang, T., Coates, A., Bissacco, A., Wu, B., and Ng, A. Y. Reading digits in natural images with unsupervised feature learning. 2011.

Pham, H., Dai, Z., Xie, Q., and Le, Q. V. Meta pseudo labels. In *Proceedings of the IEEE/CVF Conference on Computer Vision and Pattern Recognition*, pp. 11557–11568, 2021.

Rasmus, A., Berglund, M., Honkala, M., Valpola, H., and Raiko, T. Semi-supervised learning with ladder networks.

Advances in Neural Information Processing Systems, 28: 3546–3554, 2015.

Sajjadi, M., Javanmardi, M., and Tasdizen, T. Regularization with stochastic transformations and perturbations for deep semi-supervised learning. *Advances in neural information processing systems*, 29:1163–1171, 2016.

Samuli, L. and Timo, A. Temporal ensembling for semi-supervised learning. In *International Conference on Learning Representations (ICLR)*, volume 4, pp. 6, 2017.

Sohn, K., Berthelot, D., Carlini, N., Zhang, Z., Zhang, H., Raffel, C. A., Cubuk, E. D., Kurakin, A., and Li, C.-L. Fixmatch: Simplifying semi-supervised learning with consistency and confidence. *Advances in Neural Information Processing Systems*, 33, 2020.

Tarvainen, A. and Valpola, H. Mean teachers are better role models: Weight-averaged consistency targets improve semi-supervised deep learning results. In *Proceedings of the 31st International Conference on Neural Information Processing Systems*, pp. 1195–1204, 2017.

Van der Maaten, L. and Hinton, G. Visualizing data using t-sne. *Journal of machine learning research*, 9(11), 2008.

Xie, Q., Dai, Z., Hovy, E., Luong, T., and Le, Q. Unsupervised data augmentation for consistency training. *Advances in Neural Information Processing Systems*, 33, 2020a.

Xie, Q., Luong, M.-T., Hovy, E., and Le, Q. V. Self-training with noisy student improves imagenet classification. In *Proceedings of the IEEE/CVF Conference on Computer Vision and Pattern Recognition*, pp. 10687–10698, 2020b.

Xu, Y., Shang, L., Ye, J., Qian, Q., Li, Y.-F., Sun, B., Li, H., and Jin, R. Dash: Semi-supervised learning with dynamic thresholding. In *International Conference on Machine Learning*, pp. 11525–11536. PMLR, 2021.

Yang, Y. and Xu, Z. Rethinking the value of labels for improving class-imbalanced learning. In *NeurIPS*, 2020.

Zagoruyko, S. and Komodakis, N. Wide residual networks. In *British Machine Vision Conference 2016*. British Machine Vision Association, 2016.

Zhang, B., Wang, Y., Hou, W., Wu, H., Wang, J., Okumura, M., and Shinozaki, T. Flexmatch: Boosting semi-supervised learning with curriculum pseudo labeling. *Advances in Neural Information Processing Systems*, 34, 2021.

Zhou, T., Wang, S., and Bilmes, J. Time-consistent self-supervision for semi-supervised learning. In *International Conference on Machine Learning*, pp. 11523–11533. PMLR, 2020.

A. Proof of Theorem 2.1

Theorem 2.1 For a binary classification problem as mentioned above, the pseudo label Y_p has the following probability distribution:

$$\begin{aligned} P(Y_p = 1) &= \frac{1}{2}\Phi\left(\frac{\frac{\mu_2 - \mu_1}{2} - \frac{1}{\beta}\log\left(\frac{\tau}{1-\tau}\right)}{\sigma_2}\right) + \frac{1}{2}\Phi\left(\frac{\frac{\mu_1 - \mu_2}{2} - \frac{1}{\beta}\log\left(\frac{\tau}{1-\tau}\right)}{\sigma_1}\right), \\ P(Y_p = -1) &= \frac{1}{2}\Phi\left(\frac{\frac{\mu_2 - \mu_1}{2} - \frac{1}{\beta}\log\left(\frac{\tau}{1-\tau}\right)}{\sigma_1}\right) + \frac{1}{2}\Phi\left(\frac{\frac{\mu_1 - \mu_2}{2} - \frac{1}{\beta}\log\left(\frac{\tau}{1-\tau}\right)}{\sigma_2}\right), \\ P(Y_p = 0) &= 1 - P(Y_p = 1) - P(Y_p = -1), \end{aligned} \quad (15)$$

where Φ is the cumulative distribution function of a standard normal distribution. Moreover, $P(Y_p = 0) = 0$ increases as $\mu_2 - \mu_1$ gets smaller.

Proof. A sample x will be assigned pseudo label 1 if

$$\frac{1}{1 + \exp(-\beta(x - \frac{\mu_1 + \mu_2}{2}))} > \tau,$$

which is equivalent to

$$x > \frac{\mu_1 + \mu_2}{2} + \frac{1}{\beta}\log\left(\frac{\tau}{1-\tau}\right).$$

Likewise, x will be assigned pseudo label -1 if

$$\frac{1}{1 + \exp(-\beta(x - \frac{\mu_1 + \mu_2}{2}))} < 1 - \tau,$$

which is equivalent to

$$x < \frac{\mu_1 + \mu_2}{2} - \frac{1}{\beta}\log\left(\frac{\tau}{1-\tau}\right).$$

If we integrate over x , we arrive at the following conditional probabilities:

$$\begin{aligned} P(Y_p = 1|Y = 1) &= \Phi\left(\frac{\frac{\mu_2 - \mu_1}{2} - \frac{1}{\beta}\log\left(\frac{\tau}{1-\tau}\right)}{\sigma_2}\right), \\ P(Y_p = 1|Y = -1) &= \Phi\left(\frac{\frac{\mu_1 - \mu_2}{2} - \frac{1}{\beta}\log\left(\frac{\tau}{1-\tau}\right)}{\sigma_1}\right), \\ P(Y_p = -1|Y = -1) &= \Phi\left(\frac{\frac{\mu_2 - \mu_1}{2} - \frac{1}{\beta}\log\left(\frac{\tau}{1-\tau}\right)}{\sigma_1}\right), \\ P(Y_p = -1|Y = 1) &= \Phi\left(\frac{\frac{\mu_1 - \mu_2}{2} - \frac{1}{\beta}\log\left(\frac{\tau}{1-\tau}\right)}{\sigma_2}\right). \end{aligned}$$

Recall that $P(Y = 1) = P(Y = -1) = 0.5$, therefore

$$\begin{aligned} P(Y_p = 1) &= \frac{1}{2}\Phi\left(\frac{\frac{\mu_2 - \mu_1}{2} - \frac{1}{\beta}\log\left(\frac{\tau}{1-\tau}\right)}{\sigma_2}\right) + \frac{1}{2}\Phi\left(\frac{\frac{\mu_1 - \mu_2}{2} - \frac{1}{\beta}\log\left(\frac{\tau}{1-\tau}\right)}{\sigma_1}\right), \\ P(Y_p = -1) &= \frac{1}{2}\Phi\left(\frac{\frac{\mu_2 - \mu_1}{2} - \frac{1}{\beta}\log\left(\frac{\tau}{1-\tau}\right)}{\sigma_1}\right) + \frac{1}{2}\Phi\left(\frac{\frac{\mu_1 - \mu_2}{2} - \frac{1}{\beta}\log\left(\frac{\tau}{1-\tau}\right)}{\sigma_2}\right). \end{aligned}$$

Now, let's use z to denote $\mu_2 - \mu_1$, to show that $P(Y_p = 0)$ increases as $\mu_2 - \mu_1$ gets smaller, we only need to show $P(Y_p = -1) + P(Y_p = 1)$ gets bigger. We write $P(Y_p = -1) + P(Y_p = 1)$ as

$$P(Y_p = 1) + P(Y_p = -1) = \frac{1}{2}\Phi(a_1z - b_1) + \frac{1}{2}\Phi(-a_1z - b_1) + \frac{1}{2}\Phi(a_2z - b_2) + \frac{1}{2}\Phi(-a_2z - b_2),$$

where $a_1 = \frac{1}{2\sigma_1}$, $a_2 = \frac{1}{2\sigma_2}$, $b_1 = \frac{\log(\frac{\tau}{1-\tau})}{\beta\sigma_1}$, $b_2 = \frac{\log(\frac{\tau}{1-\tau})}{\beta\sigma_2}$ are positive constants. We further only need to show that $f(z) = \frac{1}{2}\Phi(a_1z - b_1) + \frac{1}{2}\Phi(-a_1z - b_1)$ is monotone increasing on $(0, \infty)$. Take the derivative of z , we have

$$f'(z) = \frac{1}{2}a_1(\phi(a_1z - b_1) - \phi(-a_1z - b_1)),$$

where ϕ is the probability density function of a standard normal distribution. Since $|a_1z - b_1| < |-a_1z - b_1|$, we have $f'(z) > 0$, and the proof is complete. \square

B. Algorithm

We present the pseudo algorithm of FreeMatch. Compared to FixMatch, each training step involves updating the global threshold and local threshold from the unlabeled data batch, and computing corresponding histograms. FreeMatchs introduce a very trivial computation budget compared to FixMatch, demonstrated also in our main paper.

Algorithm 1 FreeMatch algorithm at t -th iteration.

- 1: **Input:** Number of classes C , labeled batch $\mathcal{X} = \{(x_b, y_b) : b \in (1, 2, \dots, B)\}$, unlabeled batch $\mathcal{U} = \{u_b : b \in (1, 2, \dots, \mu B)\}$, unsupervised loss weight w_u , fairness loss weight w_f , and EMA decay λ .
- 2: Compute \mathcal{L}_s for labeled data

$$\mathcal{L}_s = \frac{1}{B} \sum_{b=1}^B \mathcal{H}(y_b, p_m(y|\omega(x_b)))$$
- 3: Update the global threshold

$$\tau_t = \lambda\tau_{t-1} + (1 - \lambda)\frac{1}{\mu B} \sum_{b=1}^{\mu B} \max(q_b)$$
 // q_b is an abbreviation of $p_m(y|\omega(u_b))$, shape of τ_t : [1]
- 4: Update the local threshold

$$\tilde{p}_t = \lambda\tilde{p}_{t-1} + (1 - \lambda)\frac{1}{\mu B} \sum_{b=1}^{\mu B} q_b$$
 // Shape of \tilde{p}_t : [C]
- 5: Update histogram for \tilde{p}_t

$$\tilde{h}_t = \lambda\tilde{h}_{t-1} + (1 - \lambda) \text{Hist}_{\mu B}(\hat{q}_b)$$
 // Shape of \tilde{h}_t : [C]
- 6: **for** $c = 1$ to C **do**
- 7: $\tau_t(c) = \text{MaxNorm}(\tilde{p}_t(c)) \cdot \tau_t$ *//* Calculate SAT
- 8: **end for**
- 9: Compute \mathcal{L}_u on unlabeled data

$$\mathcal{L}_u = \frac{1}{\mu B} \sum_{b=1}^{\mu B} \mathbb{1}(\max(q_b) \geq \tau_t(\arg \max(q_b))) \cdot \mathcal{H}(\hat{q}_b, Q_b)$$
- 10: Compute expectation of probability on unlabeled data

$$\bar{p} = \frac{1}{\mu B} \sum_{b=1}^{\mu B} \mathbb{1}(\max(q_b) \geq \tau_t(\arg \max(q_b))) Q_b$$
 // Q_b is an abbr. of $p_m(y|\Omega(u_b))$, shape of \bar{p} : [C]
- 11: Compute histogram for \bar{p}

$$\bar{h} = \text{Hist}_{\mu B}(\mathbb{1}(\max(q_b) \geq \tau_t(\arg \max(q_b))) \hat{Q}_b)$$
 // Shape of \bar{h} : [C]
- 12: Compute \mathcal{L}_f on unlabeled data

$$\mathcal{L}_f = -\mathcal{H}\left(\text{SumNorm}\left(\frac{\tilde{p}_t}{\tilde{h}_t}\right), \text{SumNorm}\left(\frac{\bar{p}}{\bar{h}}\right)\right)$$
- 13: **Return:** $\mathcal{L}_s + w_u \cdot \mathcal{L}_u + w_f \cdot \mathcal{L}_f$

C. Hyperparameter setting

For reproduction, we show the detailed hyperparameter setting for FreeMatch in Table 5 and 6, for algorithm-dependent and algorithm-independent hyperparameters, respectively.

Note that for ImageNet experiments, we used the same learning rate, optimizer scheme, and training iterations as other experiments, and a batch size of 128 is adopted, whereas, in FixMatch, a large batch size of 1024 and a different optimizer is used. From our experiments, we found that training ImageNet with only 2^{20} is not enough, and the model starts converging at the end of training. Longer training iterations on ImageNet will be explored in the future.

D. Extensive Experiment Details and Results

We present extensive experiment details and results as complementary to the experiments in the main paper.

Table 5. Algorithm dependent hyperparameters.

Algorithm	FreeMatch
Unlabeled Data to Labeled Data Ratio (CIFAR-10/100, STL-10, SVHN)	7
Unlabeled Data to Labeled Data Ratio (ImageNet)	1
Loss weight w_u for all experiments	1
Loss weight w_f for CIFAR-10 (10), CIFAR-100 (400), STL-10 (40), ImageNet (100k), SVHN	0.01
Loss weight w_f for others	0.05
Thresholding EMA decay for all experiments	0.999

Table 6. Algorithm independent hyperparameters.

Dataset	CIFAR-10	CIFAR-100	STL-10	SVHN	ImageNet
Model	WRN-28-2	WRN-28-8	WRN-37-2	WRN-28-2	ResNet-50
Weight decay	5e-4	1e-3	5e-4	5e-4	3e-4
Batch size		64			128
Learning rate			0.03		
SGD momentum			0.9		
EMA decay			0.999		

D.1. CIFAR-10 (10) Labeled Data

Following (Sohn et al., 2020), we investigate the limitations of SSL algorithms by giving only **one labeled training sample per class**. The selected 3 labeled training sets are visualized in Figure 5, which are obtained by (Sohn et al., 2020) using ordering mechanism (Carlini et al., 2019).

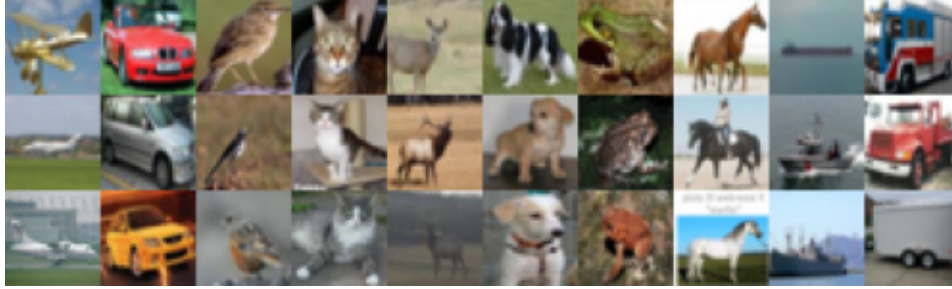


Figure 5. CIFAR-10 (10) labeled samples visualization, sorted from the most prototypical dataset (first row) to least prototypical dataset (last row).

D.2. Detailed Results

To comprehensively evaluate the performance of all methods in a classification setting, we further report the precision, recall, f1 score, and AUC (area under curve) results of CIFAR-10 with the same 10 labels, CIFAR-100 with 400 labels, SVHN with 40 labels, and STL-10 with 40 labels. As shown in Table 7 and 8, FreeMatch also has the best performance on precision, recall, F1 score, and AUC in addition to the top1 error rates reported in the main paper.

Following the evaluation protocol in the previous method (Tervainen & Valpola, 2017; Sohn et al., 2020), we also report the mean error rates of the last 20 checkpoints of all the methods in Table 9. These conclusions are in consistency with the results of Table 1 in the main paper, showing the effectiveness and robustness of FreeMatch. One may also notice that the mean error rates of the last 20 checkpoints are much lower compared to the best error rates reported in Table 1, indicating that, with our learning scheme, most algorithms overfit the training data at the end of training. We suggest future

Table 7. Precision, recall, f1 score and AUC results on CIFAR-10/100.

Datasets	CIFAR-10 (10)				CIFAR-100 (400)			
	Precision	Recall	F1 Score	AUC	Precision	Recall	F1 Score	AUC
UDA	0.5304	0.5121	0.4754	0.8258	0.5813	0.5484	0.5087	0.9475
FixMatch	0.6436	0.6622	0.6110	0.8934	0.5574	0.5430	0.4946	0.9363
Dash	0.6409	0.5410	0.4955	0.8458	0.5833	0.5649	0.5215	0.9456
MPL	0.6286	0.6857	0.6178	0.7993	0.5799	0.5606	0.5193	0.9316
FlexMatch	0.6769	0.6861	0.6780	0.9126	0.6135	0.6193	0.6107	0.9675
FreeMatch	0.8619	0.8593	0.8523	0.9843	0.6243	0.6261	0.6137	0.9692

Table 8. Precision, recall, f1 score and AUC results on SVHN and STL-10.

Datasets	SVHN (40)				STL-10 (40)			
	Precision	Recall	F1 Score	AUC	Precision	Recall	F1 Score	AUC
UDA	0.9783	0.9777	0.9780	0.9977	0.6385	0.5319	0.4765	0.8581
FixMatch	0.9731	0.9706	0.9716	0.9962	0.6590	0.5830	0.5405	0.8862
Dash	0.9782	0.9778	0.9780	0.9978	0.8117	0.6020	0.5448	0.8827
MPL	0.9564	0.9513	0.9512	0.9844	0.6191	0.5740	0.4999	0.8529
FlexMatch	0.9566	0.9691	0.9625	0.9975	0.6403	0.6755	0.6518	0.9249
FreeMatch	0.9783	0.9800	0.9791	0.9979	0.8489	0.8439	0.8354	0.9792

works report both best error rates and mean error rates for a more fair comparison since the convergence speed of different algorithms is indeed very different.

Table 9. Mean error rates of last 20 checkpoints of all methods. There are 1000 iterations between every two checkpoints

Dataset	CIFAR-10				CIFAR-100			SVHN			STL-10	
	10	40	250	4000	400	2500	10000	40	250	1000	40	1000
II Model	82.40 \pm 0.75	78.78 \pm 2.24	55.79 \pm 2.61	13.63 \pm 0.60	89.27 \pm 0.73	60.58 \pm 0.66	38.49 \pm 0.09	76.23 \pm 4.60	18.44 \pm 2.79	7.77 \pm 0.03	77.80 \pm 0.63	35.63 \pm 0.25
Pseudo Label	84.06 \pm 1.76	77.42 \pm 1.19	48.33 \pm 2.43	15.64 \pm 0.29	90.01 \pm 0.21	58.38 \pm 0.42	37.64 \pm 0.16	69.05 \pm 0.77	16.76 \pm 1.02	9.99 \pm 0.35	76.44 \pm 0.67	33.57 \pm 0.40
VAT	82.29 \pm 1.12	81.90 \pm 2.39	42.43 \pm 1.86	10.83 \pm 0.07	89.28 \pm 1.71	47.44 \pm 0.68	32.66 \pm 0.33	80.19 \pm 4.08	4.54 \pm 0.12	4.31 \pm 0.20	78.34 \pm 1.24	48.36 \pm 0.29
Mean Teacher	82.33 \pm 1.74	77.96 \pm 2.63	42.47 \pm 3.79	8.49 \pm 0.21	81.58 \pm 1.51	45.61 \pm 1.12	32.38 \pm 0.12	47.12 \pm 2.96	3.56 \pm 0.08	3.38 \pm 0.03	76.04 \pm 2.94	38.94 \pm 1.14
UDA	83.27 \pm 11.82	10.96 \pm 3.68	5.46 \pm 0.07	4.60 \pm 0.05	51.97 \pm 1.38	29.92 \pm 0.35	23.64 \pm 0.33	5.31 \pm 4.39	2.01 \pm 0.03	1.97 \pm 0.04	41.11 \pm 5.21	8.00 \pm 0.58
FixMatch	25.30 \pm 8.06	7.99 \pm 0.59	5.12 \pm 0.03	4.46 \pm 0.11	48.95 \pm 1.19	29.19 \pm 0.25	23.06 \pm 0.12	3.92 \pm 1.18	2.09 \pm 0.08	2.06 \pm 0.01	44.70 \pm 6.58	7.38 \pm 0.26
Dash	33.56 \pm 12.20	11.02 \pm 4.05	5.43 \pm 0.20	4.68 \pm 0.07	47.88 \pm 1.31	28.62 \pm 0.41	22.92 \pm 0.15	2.28 \pm 0.18	2.12 \pm 0.04	2.07 \pm 0.01	41.21 \pm 5.25	7.52 \pm 0.81
MPL	32.01 \pm 8.86	9.65 \pm 3.02	6.08 \pm 0.48	4.76 \pm 0.06	48.45 \pm 1.61	28.41 \pm 0.14	22.25 \pm 0.18	14.74 \pm 14.69	2.41 \pm 0.04	2.39 \pm 0.01	41.49 \pm 3.90	7.05 \pm 0.51
FlexMatch	17.03 \pm 16.55	5.19 \pm 0.05	5.33 \pm 0.12	4.47 \pm 0.09	45.91 \pm 1.76	28.11 \pm 0.20	23.04 \pm 0.28	20.81 \pm 5.26	17.32 \pm 2.07	12.90 \pm 2.68	44.69 \pm 7.49	6.15 \pm 0.25
FreeMatch	10.64 \pm 7.56	5.18 \pm 0.05	5.08 \pm 0.17	4.39 \pm 0.09	44.68 \pm 0.54	27.94 \pm 0.22	22.69 \pm 0.14	2.05 \pm 0.03	2.04 \pm 0.01	2.04 \pm 0.03	22.17 \pm 3.99	6.20 \pm 0.16

D.3. CIFAR-10 (10) Confusion Matrix

We plot the confusion matrix of FreeMatch and other SSL methods on CIFAR-10 (10) in Figure 6. It is worth noting that even with the least prototypical labeled data in our setting, FreeMatch still gets good results while other SSL methods fail to separate the unlabeled data into different clusters, showing inconsistency with the low-density assumption in SSL.

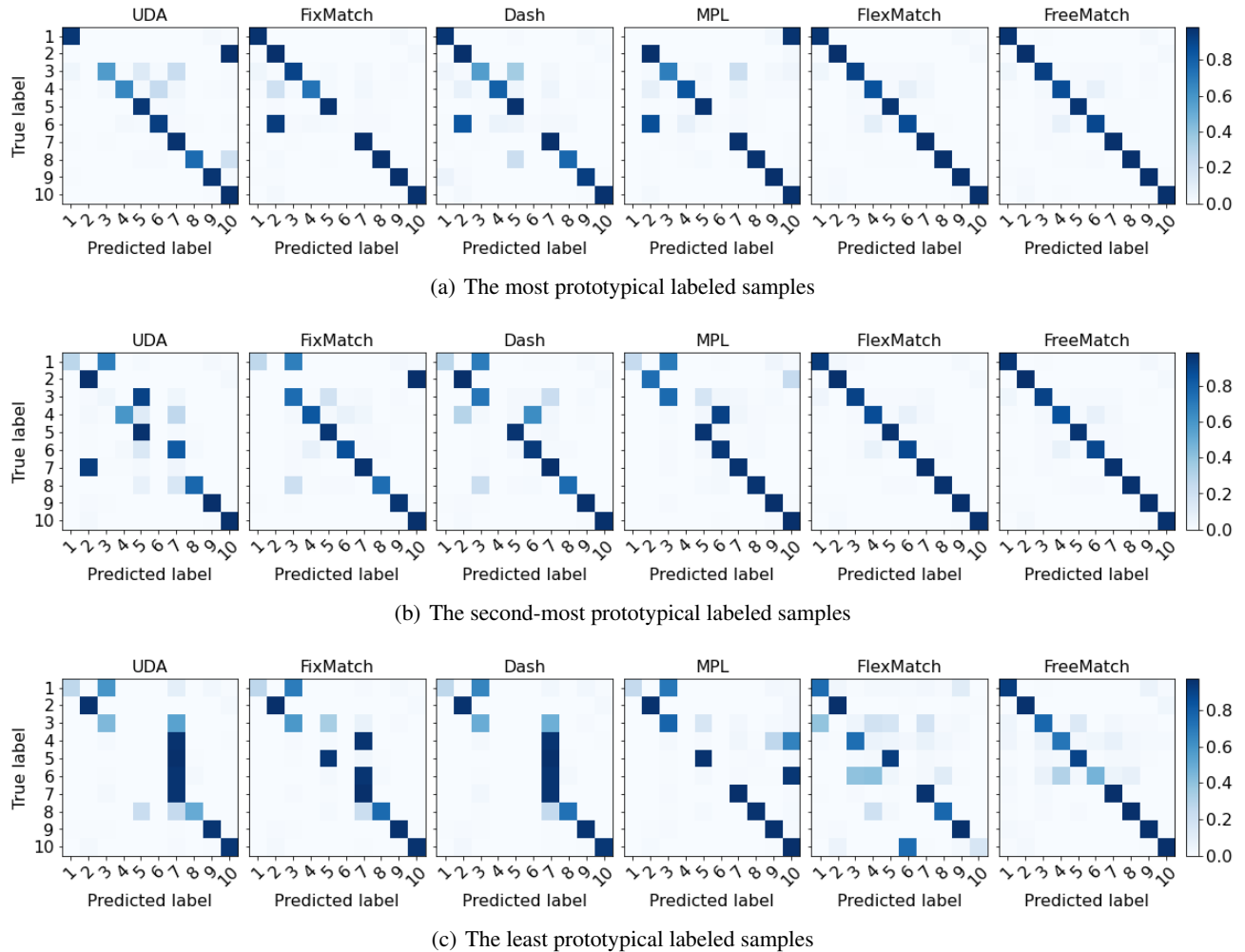


Figure 6. Confusion matrix on the test set of CIFAR-10 (10). Rows correspond to the rows in Figure 5. Columns correspond to different SSL methods.